Hindawi Publishing Corporation
Journal of Chemistry
Volume 2015, Article ID 791829, 8 pages
http://dx.doi.org/10.1155/2015/791829

Research Article

One-Step Synthesis of Spherical γ-Fe_2O_3 Nanopowders and the Evaluation of Their Photocatalytic Activity for Orange I Degradation

Chunhua Liang,[1] Hui Liu,[2] Jianmin Zhou,[2] Xiaochun Peng,[2] and Haizhou Zhang[1]

[1]*Department of Chemistry, Huaihua University, Huaihua, Hunan 418008, China*
[2]*State Environmental Protection Key Laboratory of Urban Ecological Environment Simulation and Protection, South China Institute of Environmental Sciences, Ministry of Environmental Protection, Guangzhou 510655, China*

Correspondence should be addressed to Jianmin Zhou; zhoujianmin076@gmail.com

Received 10 April 2015; Revised 27 May 2015; Accepted 15 June 2015

Academic Editor: Davide Vione

Maghemite (γ-Fe_2O_3) nanopowders were synthesized under aeration (oxidizing) conditions by aqueous synthesis in this study. The microstructures of the prepared powders were characterized by X-ray diffraction (XRD), scanning electron microscopy (SEM), and BET-BJH. The XRD analysis and the chemical experiments showed that well-crystallized γ-Fe_2O_3 nanoparticles were successfully obtained with a mean particle size of approximately 17 nm. The prepared γ-Fe_2O_3 was spherical with a BET surface area of 14.357 m^2/g and a total pore volume of 0.050 cm^3/g. Varying the reaction conditions, such as pH, temperature, and reaction time, we obtained crystallized γ-Fe_2O_3 powders with different crystallization extent and different particle sizes. When the pH of the reaction suspension was increased, the reaction time was prolonged, and the reaction temperature was increased, the γ-Fe_2O_3 powders underwent superior crystallization and had larger particle sizes. All the obtained γ-Fe_2O_3 powders had significant photocatalytic activities under both UV and visible light irradiation for Orange I degradation, and the powders with better crystallization and larger particle size had relatively lower activities for Orange I photocatalytic degradation. The one-step aqueous synthesis method presented in this paper may provide an advantageous pathway to synthesize large quantities of this important iron oxide.

1. Introduction

Recently, the synthesis of magnetic material on the ultrananoscale has been a field of intense study. Therefore, the development of monodisperse metal oxides has been intensively pursued because of their technological and fundamental importance. The syntheses of iron oxide and ferric oxide particularly attract a great deal of interest because of their application in the nanotechnologies of information storage, magnetic resonance imaging contrast agent, ferrofluids, and catalysis [1–3]. Maghemite (γ-Fe_2O_3) is one of the most historically interesting iron oxides due to its chemical stability, biocompatibility, and heating ability [4]. It is of great interest for potential applications, such as pigment, recording materials, photocatalysis, ferrofluid technology, and magnetocaloric refrigeration [5–7]. Maghemite has a structure similar to that of magnetite. It differs from magnetite in that all or most of the Fe is in the trivalent state. Cation vacancies compensate for the oxidation of Fe(II) [8].

Various preparation methods of maghemite nanoparticles, including coprecipitation, microemulsion, electrochemical synthesis, and hydrothermal synthesis, have been developed [9]. However, most of them have several problems and only a few could be used in mass production. Among the synthesis methods, hydrothermal synthesis is considered a promising candidate for the mass production of maghemite and has the following advantages [10]. (i) The maghemite particles can be obtained at a lower reaction temperature and this can prevent the agglomeration between particles. (ii) The purity of the prepared product under appropriate conditions could be high owing to recrystallization in hydrothermal solution. (iii) The equipment and processing required are simple, and the control of reaction conditions is easy. Therefore, over the past several decades, the synthesis of materials

by hydrothermal methods has been thoroughly studied. However, the disadvantages of the traditional hydrothermal method are also conspicuous. High pressures and relatively high energy costs are typically required, and uniform size powders are difficult to obtain [11]. It has been demonstrated that powders prepared by aqueous synthesis under lower temperatures are composed of much softer agglomerates that sinter much better than those prepared by calcination decomposition of the same oxides. The softer agglomerates could thus be sintered at low temperatures without the calcination and milling steps [12, 13].

In this paper, a novel aqueous process for the synthesis of spherical maghemite nanoparticles was developed by using Iron(II) chloride tetrahydrate, hexamethylenetetramine, and sodium nitrate. In the synthesis process, simple instrumentation and a one-step procedure were needed for the preparation of maghemite. Furthermore, the reaction conditions, such as temperature, pH, and reaction time, were investigated. The process described herein may be a novel, promising aqueous method for the mass preparation of maghemite nanopowders.

2. Experimental

2.1. Preparation Procedure of γ-Fe_2O_3. All of the chemicals used in this work were of analytical reagent grade from the commercial market and were used without further purification. The synthesis process was as follows: 20 g of Iron(II) chloride tetrahydrate ($FeCl_2{\cdot}4H_2O$), 26 g of hexamethylenetetramine ($(CH_2)_6N_4$), and 6 g of sodium nitrate ($NaNO_3$) were dissolved in 500, 100, and 100 mL of double-distilled water, respectively. Then, the three solutions were mixed to obtain black-green precipitate. The precipitate was aged in the mixture at 60°C for 6 h with constant oxygen pumping before it was filtered by filter paper. The precipitate remaining on the filter paper was washed three times with alcohol and distilled water to remove anions and organic impurities and then dried at 55°C for 48 h. At last, the dried sample was ground and spherical maghemite nanopowder was obtained. For the preparation of γ-Fe_2O_3 powders under different conditions, the reaction temperature, reaction time, or reaction pH was adjusted. The pH was adjusted by titrating with 0.5 M HCl solution or 0.5 M NaOH solution, while the other two corresponding reaction conditions were held constant.

2.2. Characterization Methods for the Prepared γ-Fe_2O_3 Powders. The X-ray powder diffraction patterns of maghemite were recorded on a Rigaku D/max-III A X-ray diffractometer at room temperature, operating at 30 kV and 30 mA, using a Cu Kα radiation (λ = 0.15418 nm) with the scanning rate of 12 degrees per minute and 2θ range from 10 to 70°. The specific surface areas were measured by the Brunauer-Emmett-Teller (BET) method in which the N_2 adsorption at 77 K was applied and a Carlo Erba Sorptometer was used [14]. The morphology of the magnetite was observed using scanning electron microscopy (SEM), which was conducted on a JEIL 6400 microscope operated at 15 kV. The Fourier transform infrared spectroscopy (FTIR) transmission spectra were obtained from KBr pellets on a FTIR-Bomem MB series instrument.

2.3. Photocatalytic Reactions. The photodegradation of Orange I was performed to evaluate the photocatalytic activities of the prepared γ-Fe_2O_3 powders. All photoreaction experiments were carried out in a photochemical reactor system. The system consisted of a Pyrex cylindrical reactor vessel with an effective volume of 250 mL, a cooling water jacket, two aeration inlets in the bottom, and an 8 W UVA lamp (Luzchem Research, Inc.) with the main emission at 365 nm or a 70 W high-pressure sodium lamp (Luzchem Research, Inc.) with the main emission in the range of 400–800 nm positioned axially at the center as the UV or visible light source. The reaction temperature was kept at 25 ± 1°C by cooling water, and the reaction suspension was constantly stirred by placing the reactor on a magnetic stir plate during the reaction process. The reaction suspension was prepared by adding doses of 0.4 g/L γ-Fe_2O_3 powder into 250 mL of a 20 mg/L aqueous Orange I solution. Prior to photoreaction, the suspension was magnetically stirred in the dark for 30 min to establish an adsorption/desorption equilibrium status. The aqueous reaction suspension was then irradiated under UVA light with constant aeration. At given time intervals, analytical samples were taken from the suspension and immediately centrifuged at 4500 rpm for 20 min. The supernatant was carefully transferred and stored in the dark for the analysis of the remaining Orange I at the wavelength of 481 nm on a UV-Vis spectrometer. The total organic carbon (TOC) concentration was determined by a total organic carbon analyzer (Shimadzu TOC-V CPH, Japan). All of the experiments were carried out in triplicate, and the mean values were reported and used to calculate the rate constants.

3. Results and Discussion

3.1. Preparation and Characterization of γ-Fe_2O_3 Powders. Figure 1 shows the XRD pattern for the powder prepared from a 6 h reaction at 60°C and pH of 6.0. From the XRD pattern, it can be observed that no diffraction peaks corresponding to FeO and α-Fe_2O_3 were present, based on the Joint Committee on Powder Diffraction Standards (JCPDS) data [15]. From the JCPDS data, it is clear that all of the XRD peaks are from the cubic spinel γ-Fe_2O_3 or Fe_3O_4. The XRD patterns of γ-Fe_2O_3 and Fe_3O_4 are very similar except for the differences in their corresponding "*d*" values and lattice constants [15, 16]. In the present case, the "*d*" values calculated for the XRD pattern are observed to be closer to corresponding values for the γ-Fe_2O_3 phase. Further, the lattice parameter calculated from the reflection from the (400) plane was found to be 8.354 Å, which is very close to the reported value for the γ-Fe_2O_3 phase (8.352 Å) [15, 16]. To further affirm the phase of γ-Fe_2O_3 and to discriminate it from that of Fe_3O_4, a chemical experiment was conducted by dissolving 0.1 g of the prepared powder in 100 mL of 5 M HCl under N_2-purging anoxic conditions throughout the process. After the powder was completely dissolved, the 1,10-phenanthroline method [17, 18] was applied to determine the concentration of Fe^{2+}. The results showed that there was no

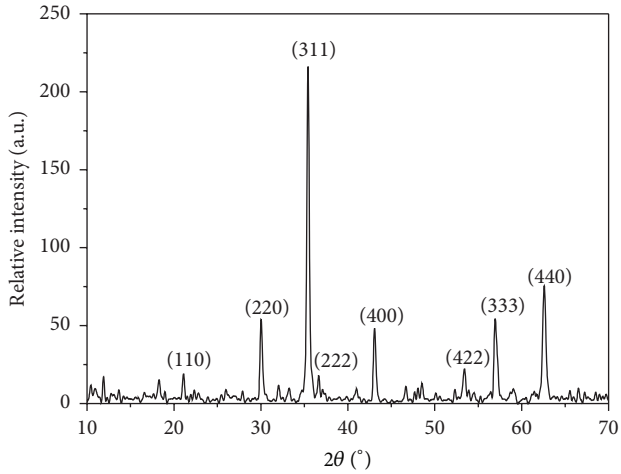

Figure 1: The XRD graph of γ-Fe_2O_3 powder prepared at 60°C and pH 6.0 for 6 h.

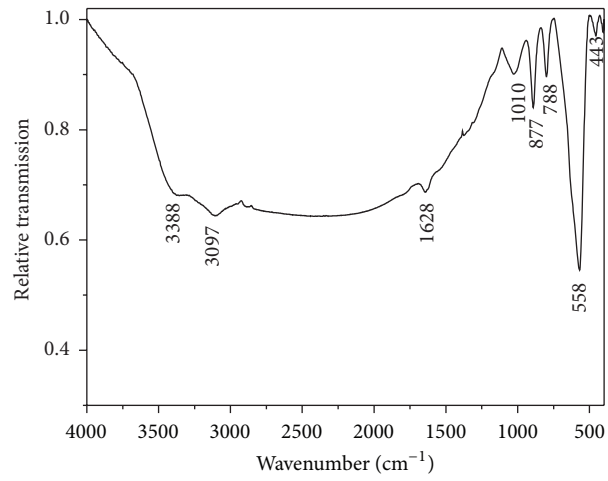

Figure 2: The FTIR spectra of γ-Fe_2O_3 powder prepared at 60°C and pH 6.0 for 6 h.

Fe^{2+} in the solution. However, when the same experimental procedure was applied to a purchased Fe_3O_4 powder, Fe^{2+} was detected. From the above XRD observations and the chemical experiments, the prepared powder was identified as γ-Fe_2O_3. The average crystallite size of the sample calculated using the Scherrer formula, $D = k\lambda(\beta\cos\theta)^{-1}$ (where $k = 0.9$, λ = wavelength of X-rays, and β = full width at half maximum of the (311) reflection), was calculated to be 17.2 nm.

Figure 2 displays the FTIR spectra of the prepared γ-Fe_2O_3. First, the broad band at 2500 cm^{-1} is attributed to both the stretching mode of the surface OH groups and the stretching modes of the water adsorbed at the surface of γ-Fe_2O_3. The infrared bands at 3388 and 3097 cm^{-1} in the FTIR spectra are due to the surface OH group vibrations, and the small band at 1628 cm^{-1} may be due to the stretching of C-H, which may exist in the residual precursor hexamethylenetetramine, or the bending of the water chemi/physisorbed at the surface of γ-Fe_2O_3. The broad structures at 1010, 877, 788, 558, and 443 cm^{-1} in the FTIR spectra are due to maghemite vibrations; at these wavenumbers, the fine-grained, synthetic maghemite shows broad IR bands in the Fe-O range [8].

To investigate the morphology of the prepared samples, SEM was employed and the resulting image of the powder prepared at 60°C for 6 h is shown in Figure 3. The image of the particles in the sample reveals a pattern with a spherical morphology that consists of nearly homogeneous grains with the average diameter of 19.5 nm, which is close to that calculated from the XRD pattern results. The BET surface area and the total pore volume, which were measured by the BET-BJH method, were 14.36 m^2/g and 0.05 cm^3/g, respectively.

3.2. Preparation of γ-Fe_2O_3 Powders under Different Conditions. To study the effect of the synthesis conditions on the properties of γ-Fe_2O_3, the powders were prepared under different pH, temperature, and reaction times. The XRD analyses of the samples prepared under different conditions

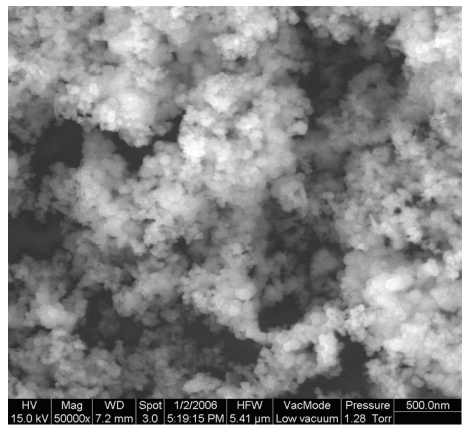

Figure 3: The SEM micrograph of γ-Fe_2O_3 powder prepared at 60°C for 6 h.

are presented in Figure 4. From Figure 4, we can see that, with the pH between 6.0 and 12.0 (Figure 4(a)), the reaction temperature between 60 and 90°C (Figure 4(b)), and the reaction time between 6 and 16 h (Figure 4(c)), well-crystallized γ-Fe_2O_3 powders could be obtained, although the powders have different degrees of crystallization and different particle sizes. These results indicate that the proposed method can synthesize crystallized γ-Fe_2O_3 powders under a very wide range of reaction conditions. The sizes of the γ-Fe_2O_3 powders prepared under pH values of 6.0, 7.0, 8.0, 9.13, 10.16, and 12.0 were 17.2, 25.8, 31.3, 41.3, 51.6, and 54.6 nm, respectively, as calculated using the Scherrer formula. The size of the γ-Fe_2O_3 powders increased with increasing reaction temperatures and prolonged reaction times. When the γ-Fe_2O_3 powders were prepared at 60, 70, 80, and 90°C, the sizes were 17.2, 34.4, 36.5, and 38.9 nm, respectively. And when the reaction times were prolonged from 6 h to 10 and 16 h, the sizes of the γ-Fe_2O_3 powders were increased from 17.2 to 22.9 and 51.6 nm, respectively.

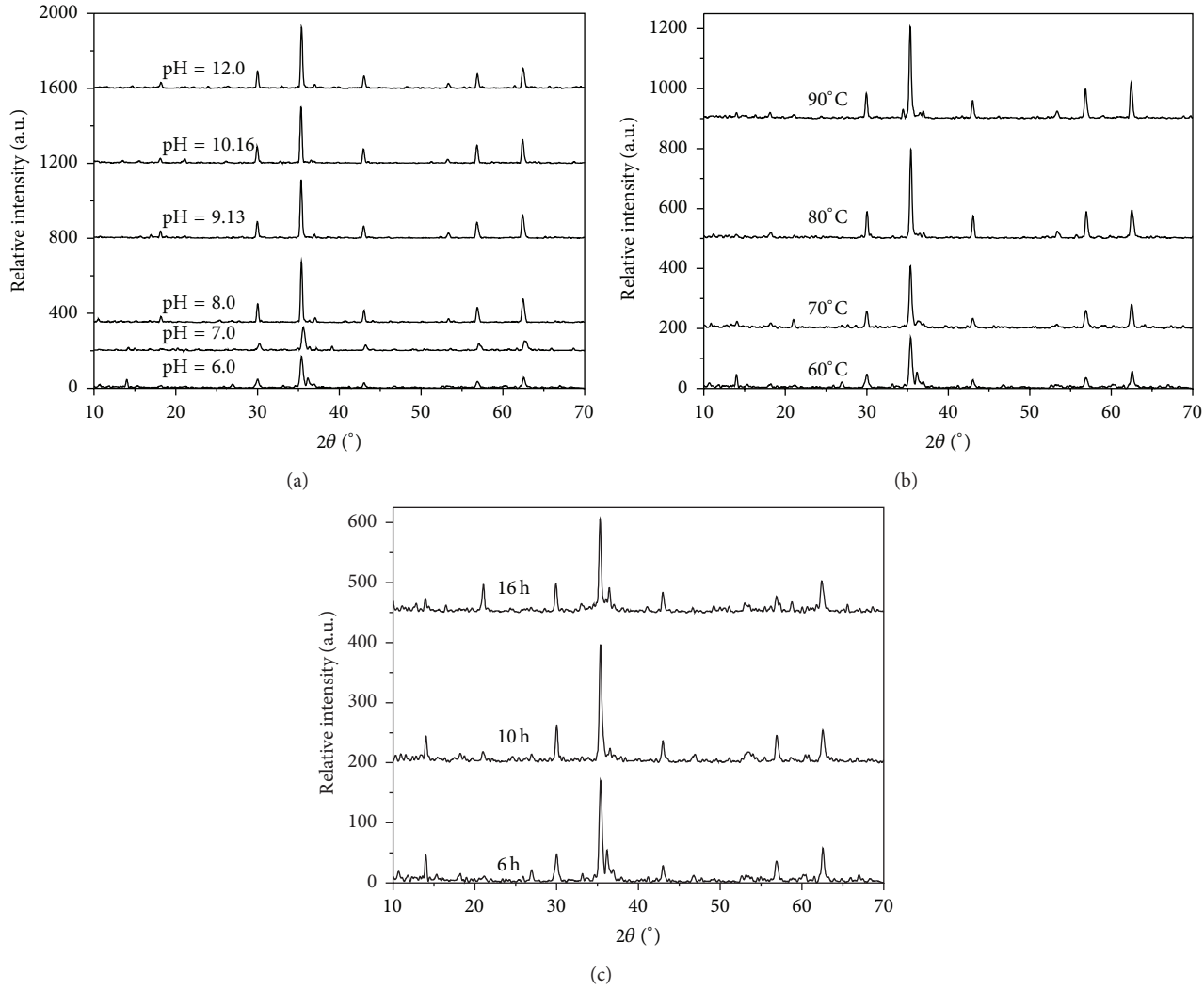

FIGURE 4: XRD patterns of γ-Fe_2O_3 powders prepared under the following conditions: (a) various pH values at 60°C for 6 h; (b) various reaction temperatures at pH of 6.0 for 6 h; (c) various reaction times at 60°C and pH of 6.0.

3.3. Evaluation of the Photocatalytic Activity of γ-Fe_2O_3 Powders. Orange I belongs to the family of azo dyes, which represent approximately 50% of all dyes used in textile industries. Azo dyes are very resistant to bacterial degradation. Therefore, common wastewater treatment cannot be employed to abate them [19]. Here, Orange I was employed to evaluate the photocatalytic activity of prepared γ-Fe_2O_3.

The photocatalytic degradation of Orange I by γ-Fe_2O_3 powders prepared at different conditions is presented in Figure 5. It is well known that photocatalytic degradation of organic compounds often follows pseudo-first-order kinetics [20, 21] and can be represented as follows:

$$-\frac{dC}{dt} = kt. \quad (1)$$

In addition, it can be integrated as

$$kt = \ln\left(\frac{C_0}{C_t}\right), \quad (2)$$

where C_0 is the initial concentration of the Orange I solution and k is the rate constant. The apparent rate constants for Orange I degradation by γ-Fe_2O_3 prepared at different conditions were calculated by (2) and listed in Table 1. From Figure 3 and Table 1 we can see that, under UVA light irradiation, Orange I could be efficiently degraded. For all of the γ-Fe_2O_3 samples prepared under different conditions, the degradation percentages of Orange I were all over 25%, and the rate constants (k) were higher than 2.2×10^{-3} min^{-1}. The γ-Fe_2O_3 prepared at pH 6.0 and 60°C for 6 h had particularly high photocatalytic activity, and the Orange I degradation percentages reached 48.89% and the k was 4.1×10^{-3} min^{-1}. The electronic structure of a semiconductor plays a key role in semiconductor photocatalysis. The band gap (E_g) of γ-Fe_2O_3 is 2.03 eV [2] and when excited by UVA light used in the experiments electrons receive energy from the photons and are thus promoted from VB to CB:

$$\gamma\text{-}Fe_2O_3 + h\upsilon \longrightarrow e^- + h^+. \quad (3)$$

Table 1: Rate constants (k) of γ-Fe_2O_3 prepared under different conditions for Orange I photodegradation.

γ-Fe_2O_3 prepared under different conditions	Rate constants (k) ($\times 10^{-3}$ min^{-1})	Relative coefficient (R^2)
Different pH values at 60°C for 6 h		
pH 6.0	4.1	0.948
pH 7.0	3.5	0.919
pH 8.0	3.2	0.942
pH 9.1	2.9	0.959
pH 10.1	2.6	0.970
pH 12.1	2.2	0.962
Different reaction temperature at pH 6.0 for 6 h		
60°C	4.1	0.948
70°C	3.9	0.959
80°C	3.7	0.959
90°C	3.4	0.971
Different reaction time at 60°C and pH 6.0		
6 h	4.1	0.948
10 h	3.1	0.951
16 h	2.6	0.981

As a dye pollutant, the self-sensitization of Orange I was also contributed to the degradation of the dye. For the model pollutant of dyes, degradation also can take place by the self-sensitization mechanism, in which the light is absorbed by the dye molecule, and charge transfer occurs from the excited dye molecule to the conduction band of the semiconductor and consequently results in the formation of an unstable dye cation radical and in parallel an active species, including $^{\bullet}O_2^-$ and $HOO^{\bullet}$, on the semiconductor surface that attacks the destabilized dye molecule [22, 23]:

$$\text{Orange I} + h\upsilon \longrightarrow \text{Orange I}^* \quad (4)$$

$$\text{Orange I}^* + \gamma\text{-}Fe_2O_3 \longrightarrow \text{Orange I}^+ + \gamma\text{-}Fe_2O_3\,(e) \quad (5)$$

$$O_2 + e^- + \gamma\text{-}Fe_2O_3\,(e) \longrightarrow {}^{\bullet}O_2^- + \gamma\text{-}Fe_2O_3 \quad (6)$$

$${}^{\bullet}O_2^- + H^+ \longrightarrow HOO^{\bullet} \quad (7)$$

For the sensitized and activated Orange I, $^{\bullet}O_2^-$ or $HOO^{\bullet}$ can act as the main active species for degradation of Orange I [24]:

$$\text{Orange I}^+ + {}^{\bullet}O_2^-\,(HOO^{\bullet}) \longrightarrow \text{peroxide or hydroxyl intermediates} \longrightarrow \text{degraded or mineralized products.} \quad (8)$$

From Figure 5, we can also see that different γ-Fe_2O_3 powders prepared under different conditions had different photocatalytic activities for Orange I degradation. For γ-Fe_2O_3 prepared under different pH values at 60°C for 6 h, the k for Orange I photocatalytic degradation followed the order of pH 6.0 > pH 7.0 > pH 8.0 > pH 9.1 > pH 10.1 > pH 12.1 (Figure 5(a)). The order of k for γ-Fe_2O_3 prepared under different reaction temperatures at pH 6.0 for 6 h was 60°C > 70°C > 80°C > 90°C (Figure 5(b)). The order of k for γ-Fe_2O_3 prepared under different reaction times at 60°C and pH 6.0 was 6 h > 10 h > 16 h (Figure 5(c)). From the above discussion, we knew that with increased reaction pH value, reaction temperature, and reaction time, the crystallization degree and particle size of the powders increased. Furthermore, with more severe reaction conditions, further conglomeration of the powders may occur. An increase in the degree of crystallization and in the particle size both would inhibit the adsorption of Orange I onto γ-Fe_2O_3 powders. Lower adsorption of organic pollutants onto the catalyst would result in lower photocatalytic degradation [21, 25]. Therefore, an increase in the reaction pH value, reaction temperature, and reaction time would result in γ-Fe_2O_3 powders with lower Orange I photocatalytic degradation activities.

Because the band gap (E_g) of γ-Fe_2O_3 is 2.03 eV and it is expected to be activated by visible light [2], the photocatalytic activities of the γ-Fe_2O_3 powders under visible light irradiation were also investigated. The photocatalytic degradation of Orange I by γ-Fe_2O_3 samples aged for different times under the irradiation of a 70 W high-pressure sodium lamp with the main emission in the range of 400–800 nm is presented in Figure 6(a). The results show that Orange I underwent degradation processes by these three γ-Fe_2O_3 samples under the irradiation of visible light, although the degradation rates were lower compared with UV light irradiation. The pseudo-first-order rate constant of Orange I degradation was 1.6×10^{-3} min^{-1} for γ-Fe_2O_3 aged for 6 h, and the k slightly decreased to 1.4×10^{-3} and 1.1×10^{-3} min^{-1} for γ-Fe_2O_3 aged for 10 and 16 h, respectively. The visible light activities of the different powders were of the same order as the activities of the UV light. To further confirm the photocatalytic activities of the obtained γ-Fe_2O_3 powders under different conditions, the mineralization of Orange I during the photocatalytic degradation was also investigated. Only the series of γ-Fe_2O_3 samples aged for different times was used in the mineralization study to evaluate the consistency with the degradation results provided in Figure 5(c). Figure 6(b) shows the TOC removal rates of Orange I after reaction for 180 min under UVA light irradiation with γ-Fe_2O_3 samples aged for different times. The results revealed that the γ-Fe_2O_3 aged for 6 h yielded the highest TOC removal (36.5%). The TOC removal rates decreased with the γ-Fe_2O_3 aged for longer periods of time and they were of the same order as the photocatalytic degradation rates of Orange I under the same light source.

4. Conclusion

Maghemite nanoparticles were synthesized by an aqueous synthesis process under oxidizing conditions. The particle size of the spherical prepared γ-Fe_2O_3 powders was approximately 17 nm. With an increase in the reaction pH value, reaction temperature, and reaction time, γ-Fe_2O_3 was successfully synthesized with better crystallization and larger

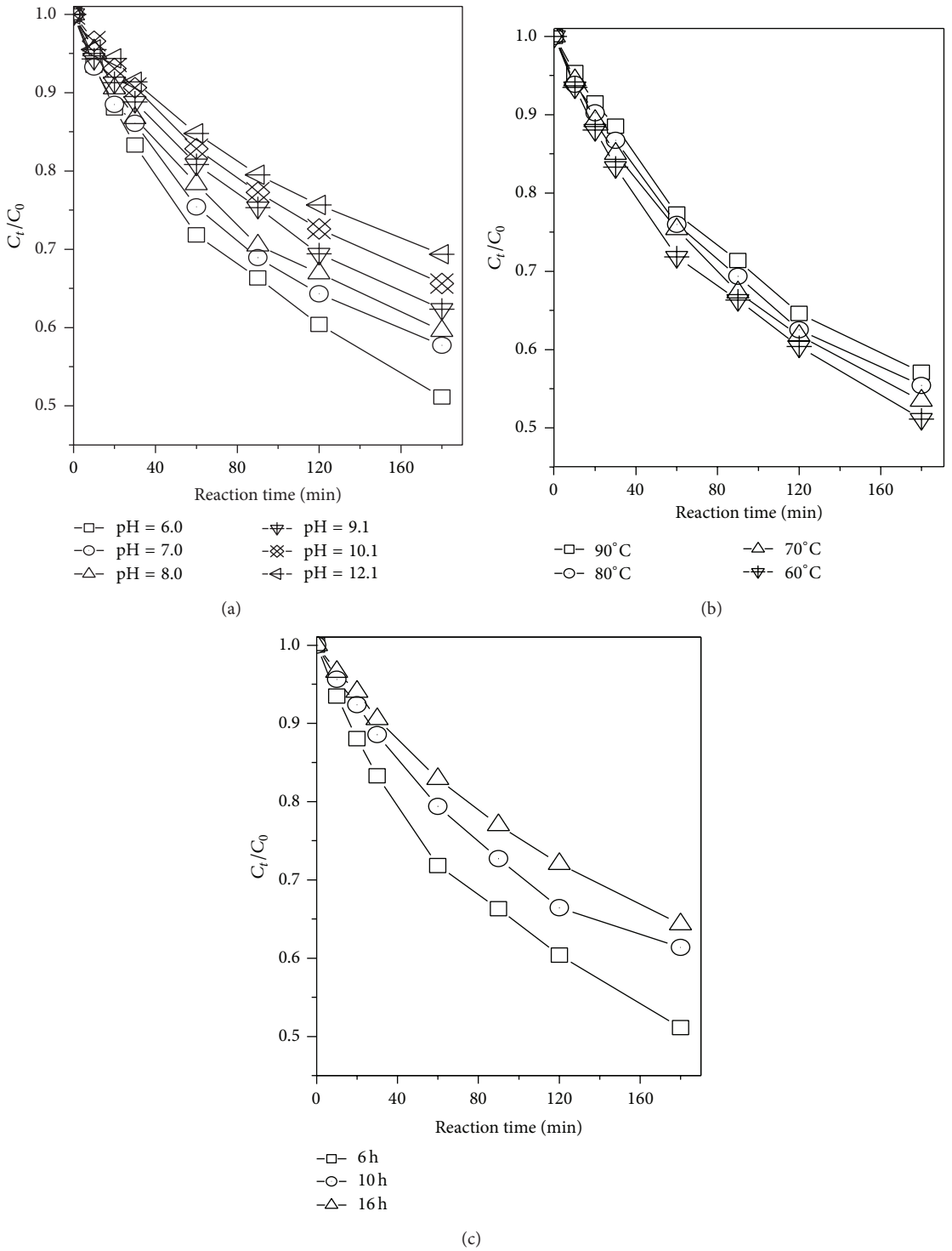

Figure 5: Photocatalytic degradation of Orange I by different γ-Fe_2O_3 powders that were prepared under the following conditions: (a) various pH values at 60°C for 6 h; (b) various reaction temperatures at pH of 6.0 for 6 h; (c) various reaction times at 60°C and pH of 6.0.

particle size. All the prepared γ-Fe_2O_3 powders had significant photocatalytic activities and achieved up to 48.89% removal and 36.5% mineralization of 20 mg/L of Orange I solutions under UV light irradiation. The γ-Fe_2O_3 powders also had visible light photoactivities for Orange I degradation. Increasing the reaction pH, prolonging the reaction time, and increasing the reaction temperatures resulted in prepared γ-Fe_2O_3 powders that had decreased photocatalytic activities. The one-step aqueous method presented in this paper offers technological, economic, and environmental advantages to the production of large quantities of maghemite from solutions.

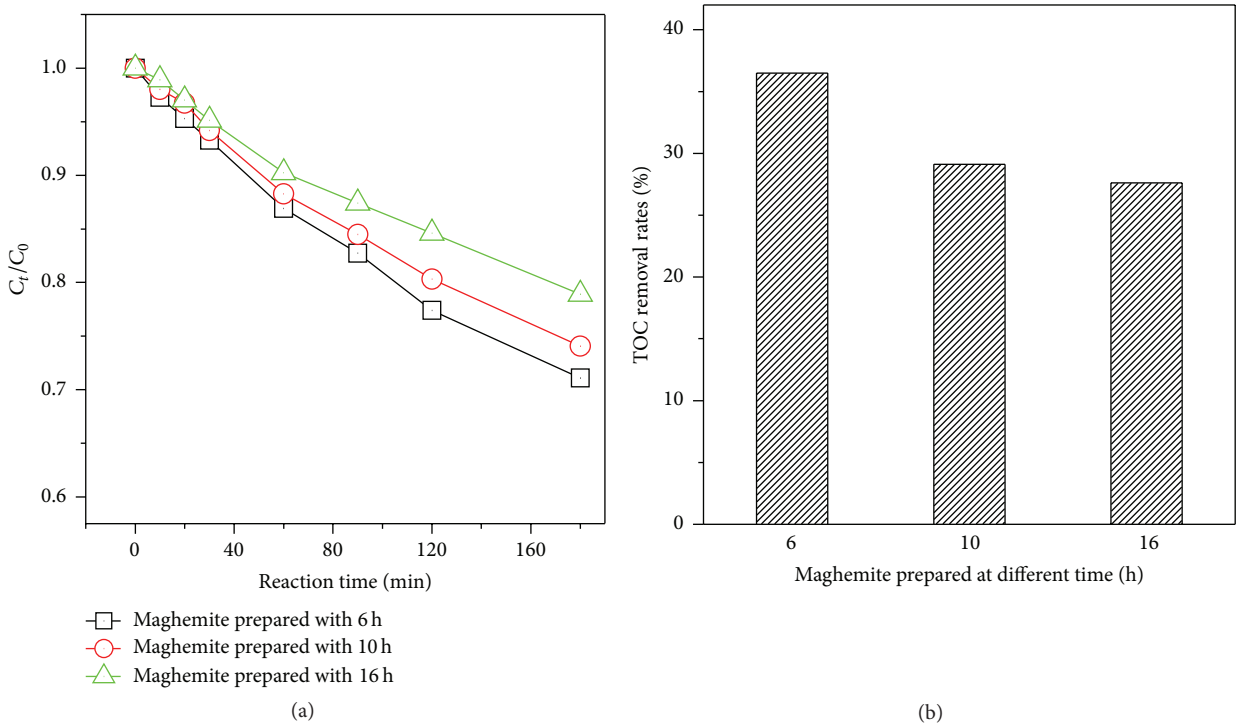

FIGURE 6: Photocatalytic degradation of Orange I by different γ-Fe_2O_3 powders that were prepared under various reaction times at 60°C and pH 6.0 (a) irradiated by visible light and (b) the TOC removal rates under irradiation of UV light.

Conflict of Interests

The authors declare that they have no conflict of interests.

Acknowledgments

This work was financially supported by the National Natural Science Foundation of China (no. 211690012) and the Scientific Research Foundation of Huaihua University. The valuable comments from two anonymous reviewers were appreciated for enhancing the paper.

References

[1] J. L. Dormann and D. Fiorani, *Magnetic Properties of Fine Particles*, Elsevier, Amsterdam, The Netherlands, 1992.

[2] J. K. Leland and A. J. Bard, "Photochemistry of colloidal semiconducting iron oxide polymorphs," *The Journal of Physical Chemistry*, vol. 91, no. 19, pp. 5076–5083, 1987.

[3] C. Liu, F. Li, X. Li, G. Zhang, and Y. Kuang, "The effect of iron oxides and oxalate on the photodegradation of 2-mercaptobenzothiazole," *Journal of Molecular Catalysis A: Chemical*, vol. 252, no. 1-2, pp. 40–48, 2006.

[4] Y.-K. Sun, M. Ma, Y. Zhang, and N. Gu, "Synthesis of nanometer-size maghemite particles from magnetite," *Colloids and Surfaces A: Physicochemical and Engineering Aspects*, vol. 245, no. 1–3, pp. 15–19, 2004.

[5] I. Anton, I. de Sabata, and L. Vékás, "Application orientated researches on magnetic fluids," *Journal of Magnetism and Magnetic Materials*, vol. 85, no. 1–3, pp. 219–226, 1990.

[6] V. Chhabra, P. Ayyub, S. Chattopadhyay, and A. N. Maitra, "Preparation of acicular γ-Fe_2O_3 particles from a microemulsion-mediated reaction," *Materials Letters*, vol. 26, no. 1-2, pp. 21–26, 1996.

[7] Y. S. Kang, S. Risbud, J. F. Rabolt, and P. Stroeve, "Synthesis and characterization of nanometer-size Fe_3O_4 and γ-Fe_2O_3 particles," *Chemistry of Materials*, vol. 8, no. 9, pp. 2209–2211, 1996.

[8] R. M. Cornell and U. Schwertmann, *The Iron Oxides: Structure, Properties, Reactions, Occurrences and Uses*, Wiley-VCH, Weinheim, Germany, 2003.

[9] I. Banerjee, Y. B. Khollam, C. Balasubramanian et al., "Preparation of γ-Fe_2O_3 nanoparticles using DC thermal arc-plasma route, their characterization and magnetic properties," *Scripta Materialia*, vol. 54, no. 7, pp. 1235–1240, 2006.

[10] D.-S. Bae, K.-S. Han, S.-B. Cho, and S.-H. Choi, "Synthesis of ultrafine Fe_3O_4 powder by glycothermal process," *Materials Letters*, vol. 37, no. 4-5, pp. 255–258, 1998.

[11] N. Liu, X. Chen, J. Zhang, and J. W. Schwank, "A review on TiO_2-based nanotubes synthesized via hydrothermal method: formation mechanism, structure modification, and photocatalytic applications," *Catalysis Today*, vol. 225, pp. 34–51, 2014.

[12] X. Wang, C. Liu, X. Li, F. Li, and S. Zhou, "Photodegradation of 2-mercaptobenzothiazole in the γ-Fe_2O_3/oxalate suspension under UVA light irradiation," *Journal of Hazardous Materials*, vol. 153, no. 1-2, pp. 426–433, 2008.

[13] M. A. Nasseri, F. Ahrari, and B. Zakerinasab, "Nickel oxide nanoparticles: a green and recyclable catalytic system for the synthesis of diindolyloxindole derivatives in aqueous medium," *RSC Advances*, vol. 5, no. 18, pp. 13901–13905, 2015.

[14] J. Yu, J. C. Yu, M. K.-P. Leung et al., "Effects of acidic and basic hydrolysis catalysts on the photocatalytic activity and microstructures of bimodal mesoporous titania," *Journal of Catalysis*, vol. 217, no. 1, pp. 69–78, 2003.

[15] Joint Committee on Powder Diffraction Standards (JCPDS), "Cards: FeO [6–711], α-Fe_2O_3 [16–653], Fe_3O_4 [19–629], γ-Fe_2O_3[39–1346]".

[16] Y. Ni, X. Ge, Z. Zhang, and Q. Ye, "Fabrication and characterization of the plate-shaped γ-Fe_2O_3 nanocrystals," *Chemistry of Materials*, vol. 14, no. 3, pp. 1048–1052, 2002.

[17] C. Paipa, M. Mateo, I. Godoy, E. Poblete, M. I. Toral, and T. Vargas, "Comparative study of alternative methods for the simultaneous determination of Fe^{+3} and Fe^{+2} in leaching solutions and in acid mine drainages," *Minerals Engineering*, vol. 18, no. 11, pp. 1116–1119, 2005.

[18] M. Chen, F. Cao, F. Li et al., "Anaerobic transformation of DDT related to iron(III) reduction and microbial community structure in paddy soils," *Journal of Agricultural and Food Chemistry*, vol. 61, no. 9, pp. 2224–2233, 2013.

[19] G. M. Atenas, E. Mielczarski, and J. A. Mielczarski, "Remarkable influence of surface composition and structure of oxidized iron layer on orange I decomposition mechanisms," *Journal of Colloid and Interface Science*, vol. 289, no. 1, pp. 171–183, 2005.

[20] C. S. Turchi and D. F. Ollis, "Photocatalytic degradation of organic water contaminants: mechanisms involving hydroxyl radical attack," *Journal of Catalysis*, vol. 122, no. 1, pp. 178–192, 1990.

[21] A. Mills, R. H. Davies, and D. Worsley, "Water purification by semiconductor photocatalysis," *Chemical Society Reviews*, vol. 22, no. 6, pp. 417–425, 1993.

[22] M. Rochkind, S. Pasternak, and Y. Paz, "Using dyes for evaluating photocatalytic properties: a critical review," *Molecules*, vol. 20, no. 1, pp. 88–110, 2015.

[23] G. Liu, X. Li, J. Zhao, S. Horikoshi, and H. Hidaka, "Photooxidation mechanism of dye alizarin red in TiO_2 dispersions under visible illumination: an experimental and theoretical examination," *Journal of Molecular Catalysis A: Chemical*, vol. 153, no. 1-2, pp. 221–229, 2000.

[24] W. S. Kuo and P. H. Ho, "Solar photocatalytic decolorization of methylene blue in water," *Chemosphere*, vol. 45, no. 1, pp. 77–83, 2001.

[25] H. Liu, M. Y. Liang, C. S. Liu, Y. X. Gao, and J. M. Zhou, "Catalytic degradation of phenol in sonolysis by coal ash and H_2O_2/O_3," *Chemical Engineering Journal*, vol. 153, no. 1–3, pp. 131–137, 2009.